PHYSICAL REVIEW D **92,** 014022 (2015)

Strong couplings of negative and positive parity nucleons to the heavy baryons and mesons

K. Azizi,[1,*] Y. Sarac,[2,†] and H. Sundu[3,‡]

[1]*Department of Physics, Doğuş University, Acıbadem-Kadıköy, 34722 Istanbul, Turkey*
[2]*Electrical and Electronics Engineering Department, Atilim University, 06836 Ankara, Turkey*
[3]*Department of Physics, Kocaeli University, 41380 Izmit, Turkey*

(Received 2 June 2015; published 20 July 2015)

The strong coupling form factors related to the strong vertices of the positive and negative parity nucleons with the heavy $\Lambda_{b[c]}[\Sigma_{b[c]}]$ baryons and heavy $B^*[D^*]$ vector mesons are calculated using a three-point correlation function. Using the values of the form factors at $Q^2 = -m^2_{\text{meson}}$, we compute the strong coupling constants among the participating particles.

DOI: 10.1103/PhysRevD.92.014022 PACS numbers: 14.20.Dh, 14.20.Lq, 14.20.Mr, 14.40.Lb

I. INTRODUCTION

The recently achieved progress in the experimental sector related to the charm and bottom baryons has provided important clues and motivations for the theoretical studies in this area. The necessity for a better understanding of the properties of these baryons such as their masses, structures, and interactions with other particles has increased the theoretical interest in them. Their various properties were studied using different methods. For instance, their masses were studied in Refs. [1–5] (see also the references therein) via various methods such as quenched lattice nonrelativistic QCD, the QCD sum rule approach within the framework of the heavy quark effective theory, the constituent quark model, QCD sum rules, and a theoretical approach based on modeling the color hyperfine interaction. References [6–19] and references therein provide some examples in which their strong and weak decays were studied.

This work provides an analysis of the strong couplings of the heavy $\Lambda_{b(c)}$ and $\Sigma_{b(c)}$ baryons to the positive parity nucleon N/negative parity nucleon N^* and heavy B^*/D^* vector meson. Here, by N^* we mean the excited $N(1535)$ nucleon with $J^P = \frac{1}{2}^-$. Such couplings occur in a low-energy regime that precludes us from the usage of the perturbative approach. The strong coupling constants are the basic parameters to determine the strength of the strong interactions among the participated particles. They also provide us a better understanding of the structure and nature of the hadrons participating in the interaction. They can also provide valuable insights to improve our understanding of the perturbative and nonperturbative nature of the strong interaction. Furthermore, these coupling constants may be useful for explanation of the observation of various exotic events by different collaborations. In addition, one may turn to these results in order to explain the properties of B^* and D^* mesons in the nuclear medium. The nucleon cloud may affect the properties of these mesons, such as their masses and decay constants in the nuclear medium, due to their interactions with nucleons (see, for instance, the Refs. [20–25]). Therefore, the present study is also helpful in identifying the properties of these particles in the nuclear medium.

Here, we calculate the strong form factors defining the strong vertices $\Lambda_b NB^*$, $\Lambda_b N^* B^*$, $\Sigma_b NB^*$, $\Sigma_b N^* B^*$, $\Lambda_c ND^*$, $\Lambda_c N^* D^*$, $\Sigma_c ND^*$, and $\Sigma_c N^* D^*$ in the framework of the QCD sum rule [26] as one of the powerful and applicable nonperturbative tools in hadron physics. By using $Q^2 = -m^2_{\text{meson}}$, we then obtain the strong coupling constants among the participating particles. This method has been previously applied to investigate some other vertices (for instance, see Refs. [6,17,27–29] and references therein).

The paper contains three sections. In the next section, we calculate the strong coupling form factors in the context of the QCD sum rule approach. Section III is devoted to the numerical analysis of the results and discussion.

II. THE STRONG COUPLING FORM FACTORS

In this section we calculate the coupling form factors defining the vertices among the hadrons under consideration using the QCD sum rule method. The starting point is to consider the following three-point correlation function:

$$\Pi_\mu(q) = i^2 \int d^4x \int d^4y e^{-ip\cdot x} e^{ip'\cdot y} \times \langle 0|\mathcal{T}(J_N(y) J^\mu_{\mathcal{M}}(0) \bar{J}_{\mathcal{B}}(x))|0\rangle, \quad (1)$$

where $\mathcal{T}$ is the time-ordering operator and $q = p - p'$ is the transferred momentum. In this equation, J_i denote the interpolating fields of different particles, $\mathcal{M}$ symbolizes the B^* or D^* meson, $\mathcal{B}$ stands for the $\Lambda_{b(c)}$ or $\Sigma_{b(c)}$ baryons, and N shows the nucleon with both parities.

*kazizi@dogus.edu.tr
†yasemin.sarac@atilim.edu.tr
‡hayriye.sundu@kocaeli.edu.tr

The three-point correlation function can be calculated both in terms of the hadronic degrees of freedom and in terms of the QCD degrees of freedom. These two different types of calculation are called the physical side and the OPE side, respectively. The results obtained from both sides are equated to acquire the QCD sum rules for the coupling form factors. For the suppression of the contributions coming from the higher states and continuum, a double Borel transformation with respect to the variables p^2 and p'^2 is applied to both sides of the obtained sum rules.

A. Physical side

For the physical side of the calculation, one inserts complete sets of appropriate $\mathcal{M}$, $\mathcal{B}$, and N hadronic states, which have the same quantum numbers as the corresponding interpolating currents, into the correlation function. Integrals over x and y give

$$\Pi_\mu^{\rm Phy}(q)=\frac{\langle 0|J_N|N(p',s')\rangle\langle 0|J^\mu_{\mathcal{M}}|\mathcal{M}(q)\rangle\langle N(p',s')\mathcal{M}(q)|\mathcal{B}(p,s)\rangle\langle\mathcal{B}(p,s)|\bar{J}_{\mathcal{B}}|0\rangle}{(p^2-m_{\mathcal{B}}^2)(p'^2-m_N^2)(q^2-m_{\mathcal{M}}^2)}+\frac{\langle 0|J_N|N^*(p',s')\rangle\langle 0|J^\mu_{\mathcal{M}}|\mathcal{M}(q)\rangle\langle N^*(p',s')\mathcal{M}(q)|\mathcal{B}(p,s)\rangle\langle\mathcal{B}(p,s)|\bar{J}_{\mathcal{B}}|0\rangle}{(p^2-m_{\mathcal{B}}^2)(p'^2-m_{N^*}^2)(q^2-m_{\mathcal{M}}^2)}+\cdots, \tag{2}$$

where $\cdots$ stands for the contributions coming from the higher states and continuum and the contributions of both positive and negative parity nucleons have been included. The matrix elements in this equation are parametrized as

$$\begin{aligned}
\langle 0|J_N|N(p',s')\rangle &= \lambda_N u_N(p',s'),\\
\langle 0|J_N|N^*(p',s')\rangle &= \lambda_{N^*}\gamma_5 u_{N^*}(p',s'),\\
\langle\mathcal{B}_{b(c)}(p,s)|\bar{J}_{\mathcal{B}_{b(c)}}|0\rangle &= \lambda_{\mathcal{B}_{b(c)}}\bar{u}_{\mathcal{B}_{b(c)}}(p,s),\\
\langle 0|J^\mu_{\mathcal{M}}|\mathcal{M}(q)\rangle &= m_{\mathcal{M}} f_{\mathcal{M}}\epsilon^*_\mu,\\
\langle N(p',s')\mathcal{M}(q)|\mathcal{B}(p,s)\rangle &= \epsilon^\nu\bar{u}_N(p',s')\left[g_1\gamma_\nu-\frac{i\sigma_{\nu\alpha}}{m_{\mathcal{B}}+m_N}q^\alpha g_2\right]u_{\mathcal{B}}(p,s),\ \langle N^*(p',s')\mathcal{M}(q)|\mathcal{B}(p,s)\rangle\\
&= \epsilon^\nu\bar{u}_{N^*}(p',s')\gamma_5\left[g_1^*\gamma_\nu-\frac{i\sigma_{\nu\alpha}}{m_{\mathcal{B}}+m_{N^*}}q^\alpha g_2^*\right]u_{\mathcal{B}}(p,s),
\end{aligned} \tag{3}$$

where $\lambda_{N(N^*)}$ and $\lambda_{\mathcal{B}}$ are the residues of the related baryons, $u_{N(N^*)}$ and $u_{\mathcal{B}}$ are the spinors for the nucleon, $\Lambda_b(\Lambda_c)$ and $\Sigma_b(\Sigma_c)$ are the baryons, and $f_{\mathcal{M}}$ represents the leptonic decay constant of $B^*(D^*)$. Here g_1 and g_2 are strong coupling form factors related to the couplings of the $\mathcal{B}$ baryon and $\mathcal{M}$ meson to the positive parity nucleon N, and g_1^* and g_2^* are those related to the strong vertices of the $\mathcal{B}$ baryon and $\mathcal{M}$ meson with the negative parity nucleon N^*. Application of the double Borel transformation with respect to the initial and final momenta squared yields

$$\hat{\mathbf{B}}\Pi_\mu^{\rm Phy}(q)=\lambda_{\mathcal{B}}f_{\mathcal{M}}e^{-\frac{m_{\mathcal{B}}^2}{M^2}}e^{-\frac{m_N^2+m_{N^*}^2}{M'^2}}[\Phi_1\gamma_\mu+\Phi_2\not{p}q_\mu+\Phi_3\not{q}p_\mu+\Phi_4\not{q}\gamma_\mu]+\cdots, \tag{4}$$

where

$$\begin{aligned}
\Phi_1 &= \frac{m_{\mathcal{M}}}{(m_{\mathcal{B}}+m_{N^*})(m_{\mathcal{M}}^2-q^2)}\left[e^{\frac{m_N^{*2}}{M'^2}}\lambda_N(g_1+g_2)(m_{\mathcal{B}}+m_{N^*})(-m_N^2+m_Nm_{\mathcal{B}}+q^2)+e^{\frac{m_N^2}{M'^2}}\lambda_{N^*}(g_1^*(m_{\mathcal{B}}+m_{N^*})\right.\\
&\left.+g_2^*(m_{\mathcal{B}}-m_{N^*}))(m_{N^*}^2+m_{N^*}m_{\mathcal{B}}-q^2)\right],\\
\Phi_2 &= \frac{1}{m_{\mathcal{M}}(m_{\mathcal{B}}+m_{N^*})(m_{\mathcal{M}}^2-q^2)}\left[e^{\frac{m_N^{*2}}{M'^2}}\lambda_N(g_1(m_N^2-m_{\mathcal{B}}^2)+g_2m_{\mathcal{M}}^2)(m_{\mathcal{B}}+m_{N^*})\right.\\
&\left.+e^{\frac{m_N^2}{M'^2}}\lambda_{N^*}(m_{\mathcal{B}}-m_{N^*})(g_1^*(m_{\mathcal{B}}+m_{N^*})^2-g_2^*m_{\mathcal{M}}^2)\right],\\
\Phi_3 &= -\frac{2m_{\mathcal{M}}}{(m_{\mathcal{M}}+m_N)(m_{\mathcal{B}}+m_{N^*})(m_{\mathcal{M}}^2-q^2)}\left[e^{\frac{m_N^{*2}}{M'^2}}\lambda_N(m_{\mathcal{B}}+m_{N^*})(g_1(m_{\mathcal{B}}+m_N)+g_2m_N)\right.\\
&\left.-e^{\frac{m_N^2}{M'^2}}\lambda_{N^*}(m_{\mathcal{B}}+m_N)(g_1^*(m_{\mathcal{B}}+m_{N^*})-g_2^*m_{N^*})\right],\\
\Phi_4 &= \frac{m_{\mathcal{B}}m_{\mathcal{M}}}{(m_{\mathcal{B}}+m_{N^*})(m_{\mathcal{M}}^2-q^2)}\left[-e^{\frac{m_N^{*2}}{M'^2}}\lambda_N(g_1+g_2)(m_{\mathcal{B}}+m_{N^*})+e^{\frac{m_N^2}{M'^2}}\lambda_{N^*}(g_1^*(m_{\mathcal{B}}+m_{N^*})+g_2^*(m_{\mathcal{B}}-m_{N^*}))\right],
\end{aligned} \tag{5}$$

with M^2 and M'^2 being the Borel mass parameters.

B. OPE side

For the OPE side of the calculation, the basic ingredients are the explicit expressions of the interpolating currents in terms of the quark fields, which are taken as

$$\begin{aligned} J_{\Lambda_{b[c]}}(x) &= \epsilon_{abc} u^{a^T}(x) C\gamma_5 d^b(x)(b[c])^c(x), \\ J_{\Sigma_{b[c]}}(x) &= \epsilon_{abc}(u^{a^T}(x) C\gamma_\nu d^b(x))\gamma_5\gamma_\nu(b[c])^c(x), \\ J_N(y) &= \epsilon_{ij\ell}(u^{i^T}(y) C\gamma_\beta u^j(y))\gamma_5\gamma_\beta d^\ell(y), \\ J_{B^*[D^*]}(0) &= \bar{u}(0)\gamma_\mu b[c](0), \end{aligned} \tag{6}$$

with C being the charge conjugation operator. By replacing these interpolating currents in Eq. (1) and doing contractions of all quark pairs via Wick's theorem, we get

$$\begin{aligned} \Pi_\mu^{\rm OPE}(q) = i^2 \int d^4x \int d^4y e^{-ip\cdot x} e^{ip'\cdot y} \epsilon_{abc}\epsilon_{ij\ell}\{&\gamma_5\gamma_\beta S_d^{cj}(y-x)\gamma_5 C S_u^{bi^T}(y-x) C\gamma_\beta S_u^{ah}(y)\gamma_\mu S_{b[c]}^{h\ell}(-x) \\ &- \gamma_5\gamma_\beta S_d^{cj}(y-x)\gamma_5 C S_u^{ai^T}(y-x) C\gamma_\beta S_u^{bh}(y)\gamma_\mu S_{b[c]}^{h\ell}(-x)\}, \end{aligned} \tag{7}$$

for $\Lambda_b N^{(*)} B^*$ and $\Lambda_c N^{(*)} D^*$ vertices and

$$\begin{aligned} \Pi_\mu^{\rm OPE}(q) = i^2 \int d^4x \int d^4y e^{-ip\cdot x} e^{ip'\cdot y} \epsilon_{abc}\epsilon_{ij\ell}\{&\gamma_5\gamma_\beta S_d^{cj}(y-x)\gamma_\nu C S_u^{bi^T}(y-x) C\gamma_\beta S_u^{ah}(y)\gamma_\mu S_{b[c]}^{h\ell}(-x)\gamma_\nu\gamma_5 \\ &- \gamma_5\gamma_\beta S_d^{cj}(y-x)\gamma_\nu C S_u^{ai^T}(y-x) C\gamma_\beta S_u^{bh}(y)\gamma_\mu S_{b[c]}^{h\ell}(-x)\gamma_\nu\gamma_5\} \end{aligned} \tag{8}$$

for the $\Sigma_b N^{(*)} B^*$ and $\Sigma_c N^{(*)} D^*$ vertices. In these equations, $S_{b[c]}^{ij}(x)$ and $S_{u[d]}^{ij}(x)$ correspond to the heavy and light quark propagators, respectively. The heavy quark propagator in the coordinate space is used as [30]

$$S_{b[c]}^{ij}(x) = \frac{i}{(2\pi)^4}\int d^4k e^{-ik\cdot x}\left\{\frac{\delta_{ij}}{\not k - m_{b[c]}} - \frac{g_s G_{ij}^{\alpha\beta}}{4}\frac{\sigma_{\alpha\beta}(\not k + m_{b[c]}) + (\not k + m_{b[c]})\sigma_{\alpha\beta}}{(k^2 - m_{b[c]}^2)^2} + \frac{\pi^2}{3}\left\langle\frac{\alpha_s GG}{\pi}\right\rangle\delta_{ij} m_{b[c]}\frac{k^2 + m_{b[c]}\not k}{(k^2 - m_{b[c]}^2)^4} + \cdots\right\}, \tag{9}$$

where we take the heavy quark mass to be finite and do not use any approximation. For the light quark propagator, we use [30]

$$S_q^{ij}(x) = i\frac{\not x}{2\pi^2 x^4}\delta_{ij} - \frac{m_q}{4\pi^2 x^2}\delta_{ij} - \frac{\langle\bar{q}q\rangle}{12}\left(1 - i\frac{m_q}{4}\not x\right)\delta_{ij} - \frac{x^2}{192}m_0^2\langle\bar{q}q\rangle\left(1 - i\frac{m_q}{6}\not x\right)\delta_{ij} - \frac{ig_s G_{\theta\eta}^{ij}}{32\pi^2 x^2}[\not x\sigma^{\theta\eta} + \sigma^{\theta\eta}\not x] + \cdots, \tag{10}$$

where q is either a u or d quark. Using these propagators in Eqs. (7) and (8), we get the OPE sides of different vertices in coordinate space, after which we perform Fourier transformations to go to the momentum space. For this, first we use

$$\frac{1}{[A^2]^n} = \int\frac{d^Dt}{(2\pi)^D} e^{-it\cdot A} i(-1)^{n+1} 2^{D-2n}\pi^{D/2}\frac{\Gamma(D/2-n)}{\Gamma(n)}\left(-\frac{1}{t^2}\right)^{D/2-n} \tag{11}$$

in the D dimension. Then, the four-integrals over x and y are performed after the replacements $x_\mu \to i\frac{\partial}{\partial p_\mu}$ and $y_\mu \to -i\frac{\partial}{\partial p'_\mu}$. This procedure brings two Dirac Deltas that are used in performing other two integrals existing in the calculations. Finally, the Feynman parametrization and the formula

$$\int d^4t\frac{(t^2)^\beta}{(t^2+L)^\alpha} = \frac{i\pi^2(-1)^{\beta-\alpha}\Gamma(\beta+2)\Gamma(\alpha-\beta-2)}{\Gamma(2)\Gamma(\alpha)[-L]^{\alpha-\beta-2}} \tag{12}$$

are used to perform the last four-integral. After lengthy calculations (see also Refs. [28,29]), we get

$$\Pi_\mu^{\rm OPE}(q) = \Pi_1(q^2)\gamma_\mu + \Pi_2(q^2)\not{p}q_\mu + \Pi_3(q^2)\not{q}p_\mu + \Pi_4(q^2)\not{q}\gamma_\mu + \text{other structures}, \tag{13}$$

where the $\Pi_i(q^2)$ functions contain contributions coming from both the perturbative and nonperturbative parts and are given as

$$\Pi_i(q^2) = \int ds \int ds' \frac{\rho_i^{\rm pert}(s,s',q^2) + \rho_i^{\rm non-pert}(s,s',q^2)}{(s-p^2)(s'-p'^2)}. \tag{14}$$

The spectral densities $\rho_i(s,s',q^2)$ appearing in this equation are obtained from the imaginary parts of the Π_i functions as $\rho_i(s,s',q^2) = \frac{1}{\pi} Im[\Pi_i]$. Here, as examples, only the results of the spectral densities corresponding to the Dirac structure γ_μ for the $\Lambda_b N B^*$ vertex are presented, which are

$$\begin{aligned}
\rho_1^{\rm pert}(s,s',q^2) = {} & \frac{m_b m_u s'^2}{64\pi^4 \mathcal{Q}} \Theta[L_1(s,s',q^2)] + \int_0^1 dx \int_0^{1-x} dy \frac{1}{64\pi^4 \mathcal{X}^3} \{m_b^4 x^2 (\mathcal{X}' + 2x) \\
& \times (\mathcal{X} + y) + q^4 xy[3y(\mathcal{X}' - 1)\mathcal{X}'(\mathcal{X}' + 4x) - 2\mathcal{X}'^2(3x + \mathcal{X}') + 2y^2(15x^2 - 14x + 2)] \\
& - 2q^2 \mathcal{X}[xy\mathcal{X}'(s(2 + 15x^2 - 18x) - s'(\mathcal{X}' - 3)) + y^2(2sx(1 - 10x + 15x^2) \\
& - 4sx^2\mathcal{X}'^2 - s'(1 - 21x + 41x^2 - 15x^3)) + s'y^3(1 - 17x + 30x^2) - 4sx^2\mathcal{X}'^2] \\
& + m_b^3 x(m_u(3 - 5x + 2x^2 - 2xy) + 3m_d(\mathcal{X}' + x)\mathcal{X}) + \mathcal{X}^2[s'^2 y(5y - 8x\mathcal{X}' \\
& - 34xy - 6y^2 + 15x^2 y + 30xy^2) + 3s^2 x^2(1 - 4y - 6x + 5x^2 + 10xy) + 2ss'x \\
& \times (5y - 9y^2 - 4x\mathcal{X}' + 15x^2 y - 26xy + 30xy^2)] + 2m_b^2 x[q^2(3x\mathcal{X}' - 3y + 16xy \\
& + 8x^2 y - 4y^2 + 16xy^2) + \mathcal{X}(s'(3y - 3x\mathcal{X}' - 16y + 8xy - 4y^2 + 16xy^2) \\
& + 2sx(1 - 3y - 5x + 4x^2 + 8xy))] + m_b[3m_d\mathcal{X}(sx\mathcal{X}(\mathcal{X}' - 1) + y(s'u - q^2 x) \\
& \times (3y - 1)) + m_u(sx\mathcal{X}(6 - 9x + 3x^2 - 3xy) + y(q^2 x(4x - 3x^2 + 3xy + y - 1) \\
& + 3s'\mathcal{X}\mathcal{X}'^2 - 3s'y\mathcal{X}(\mathcal{X}' + 2)))]\}\Theta[L_2(s,s',q^2)],
\end{aligned} \tag{15}$$

and

$$\begin{aligned}
\rho_1^{\rm non-pert}(s,s',q^2) = {} & \frac{\langle u\bar{u}\rangle}{16\pi^2 \mathcal{Q}}[s'(m_u - 2m_b) - q^2 m_d]\Theta[L_1(s,s',q^2)] \\
& + \int_0^1 dx \int_0^{1-x} dy \frac{1}{8\pi^2 \mathcal{X}}[\langle d\bar{d}\rangle(m_d(2x + \mathcal{X}')\mathcal{X} - m_b(x + \mathcal{X}\mathcal{X}') - m_u\mathcal{X}) \\
& + \langle u\bar{u}\rangle(m_u(3xy + 3x\mathcal{X}' - y) - m_b(x + \mathcal{X}') - 2m_d\mathcal{X})]\Theta[L_2(s,s',q^2)] \\
& - \left\langle \alpha_s \frac{G^2}{\pi} \right\rangle \frac{1}{1152\pi^2 \mathcal{Q}^4}[9m_b\mathcal{Q}^3(m_d - 2m_u) + s'\mathcal{Q}^2(3m_b(m_d + m_u) + 2q^2) \\
& + 3s'^2(m_b^4 - 2q^2 m_b(m_b - m_u) + q^4)]\Theta[L_1(s,s',q^2)] \\
& + \int_0^1 dx \int_0^{1-x} dy \left\langle \alpha_s \frac{G^2}{\pi} \right\rangle \frac{1}{192\pi^2 \mathcal{X}^3}[3\mathcal{X}'^3(2x + \mathcal{X}') + y^2(15 + x(39\mathcal{X}' - 20)) \\
& + y(2x + \mathcal{X}') + \mathcal{X}'(11\mathcal{X}' - 1) + 6y^3(2x + \mathcal{X}')]\Theta[L_2(s,s',q^2)] \\
& - \frac{1}{192\pi^2 \mathcal{Q}}[m_0^2\langle d\bar{d}\rangle(6m_b + 4m_d) + m_0^2\langle u\bar{u}\rangle(7m_u - 3m_d - 18m_b)]\Theta[L_1(s,s',q^2)],
\end{aligned} \tag{16}$$

where

$$\begin{aligned}
\mathcal{X} &= x + y - 1, \\
\mathcal{X}' &= x - 1, \\
\mathcal{Q} &= m_b^2 - q^2, \\
L_1(s,s',q^2) &= s', \\
L_2(s,s',q^2) &= -m_b^2 x + sx - sx^2 + s'y + q^2 xy - sxy - s'xy - s'y^2.
\end{aligned} \tag{17}$$

The $\Theta[\ldots]$ in these equations is the unit-step function. As already stated, the match of the results obtained from the physical and OPE sides of the correlation function gives the QCD sum rules for the strong coupling form factors. As examples, for the form factors related to the $\Lambda_b N B^*$ and $\Lambda_b N^* B^*$ vertices, we get

$$
\begin{aligned}
g_1(q^2) &= e^{\frac{m_{\Lambda_b}^2}{M^2}} e^{\frac{m_N^2}{M'^2}} \frac{(m_{B^*}^2 - q^2)}{\lambda_N \mathcal{H}} \{ m_{B^*}^2 [m_{\Lambda_b}^4 (\Pi_3 - 2\Pi_2) - 2\mathcal{V} m_N m_{N^*} \Pi_4 - 2m_{\Lambda_b}^3 (m_{N^*}\Pi_2 + \Pi_4) \\
&+ m_{\Lambda_b}(2q^2\Pi_4 + (m_N^2 - m_N m_{N^*})(m_{N^*}\Pi_3 + 2\Pi_4)) \\
&- m_{\Lambda_b}^2 (m_N m_{N^*}(2\Pi_2 - \Pi_3) + m_{N^*}^2 \Pi_3 + m_N^2 (\Pi_3 - 2\Pi_2) + 2m_{N^*}\Pi_4 - 2\Pi_1)] \\
&+ (m_{\Lambda_b} - m_{N^*})(m_{\Lambda_b} + m_{N^*})[m_{\Lambda_b} m_N m_{N^*} \mathcal{V}\Pi_3 - 2m_N m_{N^*}\mathcal{V}\Pi_4 + m_{\Lambda_b}^4 \Pi_3 + 2q^2 m_{\Lambda_b}\Pi_4 \\
&+ m_{\Lambda_b}^2 (2\Pi_1 - (m_N \mathcal{V} + m_{N^*}^2)\Pi_3)]\}, \\
g_2(q^2) &= e^{\frac{m_{\Lambda_b}^2}{M^2}} e^{\frac{m_N^2}{M'^2}} \frac{(m_{B^*}^2 - q^2)(m_N + m_{\Lambda_b})}{\lambda_N \mathcal{H}} \{ -m_{\Lambda_b}^5 \Pi_3 + m_N m_{\Lambda_b}^4 \Pi_3 + m_{\Lambda_b} m_{N^*}^3 \mathcal{V}\Pi_3 \\
&+ m_{N^*} m_{\Lambda_b}^3 (2m_{N^*}\Pi_3 - m_N \Pi_3 - 2\Pi_4) + 2m_{\Lambda_b}(m_N(m_{N^*}^2 - q^2) + m_{N^*} q^2)\Pi_4 - 2m_{N^*}^3 \mathcal{V}\Pi_4 \\
&+ m_{B^*}^2 (m_{\Lambda_b} - \mathcal{V})(m_{\Lambda_b}(2m_{\Lambda_b}\Pi_2 - m_{\Lambda_b}\Pi_3 + m_{N^*}\Pi_3) + 2(m_{\Lambda_b} - m_{N^*})\Pi_4) \\
&- m_{\Lambda_b}^2 (m_{N^*}(m_N m_{N^*}\Pi_3 - 4m_N \Pi_4 + 4m_{N^*}\Pi_4) + 2\mathcal{V}\Pi_1)\}, \\
g_1^*(q^2) &= e^{\frac{m_{\Lambda_b}^2}{M^2}} e^{\frac{m_N^2}{M'^2}} \frac{(m_{B^*}^2 - q^2)}{\lambda_{N^*} \mathcal{H}} \{ (m_{\Lambda_b} - m_N)(m_{\Lambda_b} + m_N)[m_{\Lambda_b}^4 \Pi_3 + m_{\Lambda_b} m_N m_{N^*} \mathcal{V}\Pi_3 \\
&+ 2m_N m_{N^*}\mathcal{V}\Pi_4 + 2m_{\Lambda_b} q^2 \Pi_4 + m_{\Lambda_b}^2 (2\Pi_1 - (m_N \mathcal{V} + m_{N^*}^2)\Pi_3)] \\
&+ m_{B^*}^2 [m_N m_{N^*} m_{\Lambda_b}\mathcal{V}\Pi_3 + 2m_{\Lambda_b}^3 (m_N \Pi_2 - \Pi_4) - 2m_N m_{N^*}\mathcal{V}\Pi_4 \\
&+ m_{\Lambda_b}^4 (\Pi_3 - 2\Pi_2) - 2m_{\Lambda_b}(m_{N^*}\mathcal{V} - q^2)\Pi_4 + m_{\Lambda_b}^2 (m_{N^*}^2 (2\Pi_2 - \Pi_3) - m_N^2 \Pi_3 \\
&+ m_N (2\Pi_4 + m_{N^*}\Pi_3 - 2m_{N^*}\Pi_2) + 2\Pi_1)]\}, \\
g_2^*(q^2) &= e^{\frac{m_{\Lambda_b}^2}{M^2}} e^{\frac{m_N^2}{M'^2}} \frac{(m_{B^*}^2 - q^2)(m_{\Lambda_b} + m_{N^*})}{\lambda_{N^*} \mathcal{H}} \{ (m_{\Lambda_b}^5 + m_{\Lambda_b} m_N^3 \mathcal{V} + m_{\Lambda_b}^4 m_{N^*})\Pi_3 + m_{\Lambda_b}^3 m_N \\
&\times ((\mathcal{V} - m_N)\Pi_3 - 2\Pi_4) - 2m_N^3 \mathcal{V}\Pi_4 + 2m_{\Lambda_b}(m_N^2 m_{N^*} + q^2 \mathcal{V})\Pi_4 - m_{B^*}^2 (m_{\Lambda_b} - \mathcal{V}) \\
&\times [m_{\Lambda_b}(2m_{\Lambda_b}\Pi_2 - (m_{\Lambda_b} + m_N)\Pi_3) + 2(m_{\Lambda_b} + m_N)\Pi_4] - m_{\Lambda_b}^2 [m_N (m_N m_{N^*}\Pi_3 \\
&- 4m_N \Pi_4 + 4m_{N^*}\Pi_4) - 2\mathcal{V}\Pi_1]\},
\end{aligned}
\tag{18}
$$

where

$$
\begin{aligned}
\mathcal{H} &= 2 f_{B^*} \lambda_{\Lambda_b} m_{B^*} m_{\Lambda_b}^2 (m_{\Lambda_b} - \mathcal{V})(m_N + m_{N^*})(m_{B^*}^2 + m_{\Lambda_b}^2 - m_N m_{\Lambda_b} - m_N^2 + m_{N^*}(m_N + m_{\Lambda_b}) - m_{N^*}^2), \\
\mathcal{V} &= (m_N - m_{N^*}).
\end{aligned}
\tag{19}
$$

III. NUMERICAL RESULTS

To numerically analyze the sum rules for the strong coupling form factors and to find their behavior with respect to $Q^2 = -q^2$, we need some inputs as presented in Table I. Besides, we also need to determine the working regions corresponding to the four auxiliary parameters, M^2, M'^2, s_0 and s_0'. The M^2 and M'^2 emerge from the double Borel transformation and s_0 and s_0' originate from continuum subtraction. These are auxiliary parameters; therefore, we need a region of them through which the strong coupling form factors have weak dependency on these parameters. The continuum thresholds are in relation to the first excited states in the initial and final channels. To determine them the energy that characterizes the beginning of the continuum is considered. Table II presents intervals of the continuum thresholds used in the calculations. To determine the working regions for the Borel mass parameters, we need to take into account the criteria that the contributions of the higher states and continuum are sufficiently suppressed and the contributions of the operators with higher dimensions are small. The intervals obtained based on these considerations are also given in Table II. As an example, we show the dependence of the

TABLE I. Input parameters used in the calculations.

Parameters	Values
$\langle\bar{u}u\rangle(1\text{ GeV}) = \langle\bar{d}d\rangle(1\text{ GeV})$	$-(0.24 \pm 0.01)^3$ GeV^3 [31]
$\langle\frac{\alpha_s G^2}{\pi}\rangle$	(0.012 ± 0.004) GeV^4 [32]
$m_0^2(1\text{ GeV})$	(0.8 ± 0.2) GeV^2 [32]
m_b	(4.18 ± 0.03) GeV [33]
m_c	(1.275 ± 0.025) GeV [33]
m_d	$4.8^{+0.5}_{-0.3}$ MeV [33]
m_u	$2.3^{+0.7}_{-0.5}$ MeV [33]
m_{B^*}	(5325.2 ± 0.4) MeV [33]
m_{D^*}	(2006.96 ± 0.10) MeV [33]
m_N	$(938.272046 \pm 0.000021)$ MeV [33]
m_{N^*}	$1525TO1535$ MeV [33]
m_{Λ_b}	(5619.5 ± 0.4) MeV [33]
m_{Λ_c}	(2286.46 ± 0.14) MeV [33]
m_{Σ_b}	(5811.3 ± 1.9) MeV [33]
m_{Σ_c}	(2452.9 ± 0.4) MeV [33]
f_{B^*}	$(210.3^{+0.1}_{-1.8})$ MeV [34]
f_{D^*}	$(241.9^{+10.1}_{-12.1})$ MeV [34]
λ_N^2	0.0011 ± 0.0005 GeV^6 [35]
λ_{N^*}	0.019 ± 0.0006 GeV^3 [36]
λ_{Λ_b}	$(3.85 \pm 0.56)10^{-2}$ GeV^3 [37]
λ_{Σ_b}	(0.062 ± 0.018) GeV^3 [38]
λ_{Λ_c}	$(3.34 \pm 0.47)10^{-2}$ GeV^3 [37]
λ_{Σ_c}	(0.045 ± 0.015) GeV^3 [38]

strong coupling form factor $g_{1_{\Lambda_b NB^*}}$ on M^2 and M'^2 at fixed values of Q^2, s_0 and s_0' in Fig. 1. From this figure we see that the dependence of the coupling form factor $g_{1_{\Lambda_b NB^*}}$ on the Borel parameters is weak at their working intervals.

In this part, we use the working regions of auxiliary parameters together with the other inputs to obtain the variation of the coupling form factors in terms of Q^2. Our calculations show that the couplings are truncated at some points and we need to extrapolate the results to the regions that the strong coupling constants are calculated. For this purpose, the following fit functions are used:

(i) fit function 1

$$g_{\mathcal{BNM}}(Q^2) = c_1 + c_2 \exp\left[-\frac{Q^2}{c_3}\right], \quad (20)$$

(ii) fit function 2

$$g_{\mathcal{BNM}}(Q^2) = \frac{g_0}{1 - a\frac{Q^2}{m_{\mathcal{B}}^2} + b(\frac{Q^2}{m_{\mathcal{B}}^2})^2}, \quad (21)$$

(iii) fit function 3

$$g_{\mathcal{BNM}}(Q^2) = B_0 + B_1 Q^2 + B_2 (Q^2)^2, \quad (22)$$

where c_1, c_2, c_3, g_0, a, b, B_0, B_1, and B_2 for different vertices are given in Tables III–XIV. To see how the above functions fit to the QCD sum rule results in reliable regions and how they differ from each other in the extrapolated region, we depict the dependence of, for instance, $g_{1_{\Lambda_b NB^*}}(Q^2)$ on Q^2 at fixed values of the auxiliary parameters and for all fit functions in Fig. 2. From this figure we see that all parametrizations fit well the sum rule results, but differ slightly from each other at the extrapolated region. The fit functions are used to attain the coupling constants at $Q^2 = -m_{\mathcal{M}}^2$ for all structures. The results for different coupling constants and different fit functions are presented in Tables XV–XVII. The presented errors in the results arise due to the uncertainties of the input parameters as well as uncertainties coming from the determination of the working regions of the auxiliary parameters. From these tables we see that the results obtained via different fit functions over all are close to each other, although we see some small differences in some values obtained using

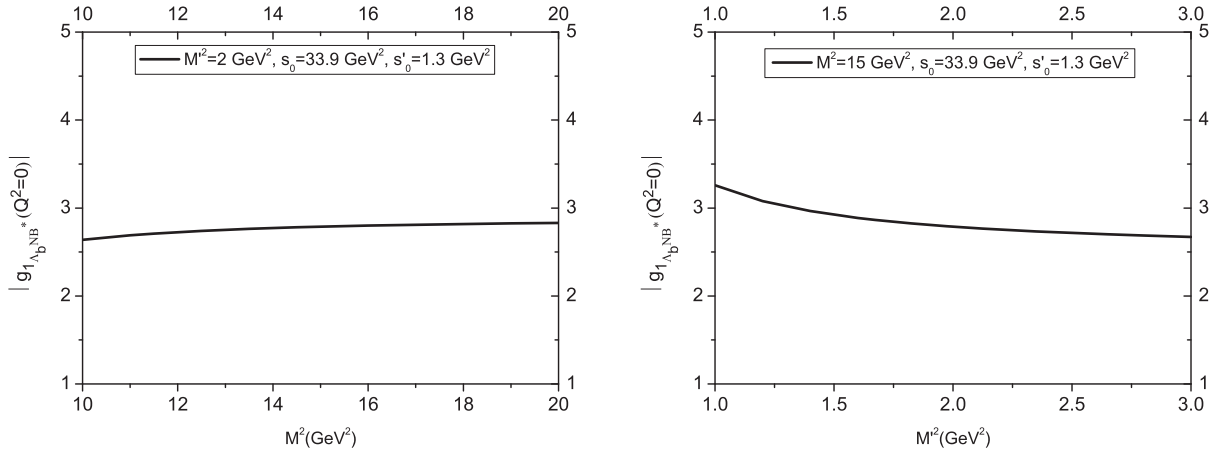

FIG. 1. Left: $g_{1_{\Lambda_b NB^*}}(Q^2 = 0)$ as a function of M^2. Right: $g_{1_{\Lambda_b NB^*}}(Q^2 = 0)$ as a function of M'^2.

TABLE II. Working intervals for auxiliary parameters.

Vertex	$s_0(\mathrm{GeV}^2)$	$s_0'(\mathrm{GeV}^2)$	$M^2(\mathrm{GeV}^2)$	$M'^2(\mathrm{GeV}^2)$
$\Lambda_b N^{(*)} B^*$	$32.71 \leq s_0 \leq 35.04$	$1.04 \leq s_0' \leq 1.99$	$10 \leq M^2 \leq 20$	$1 \leq M'^2 \leq 3$
$\Sigma_b N^{(*)} B^*$	$34.91 \leq s_0 \leq 37.40$	$1.04 \leq s_0' \leq 1.99$	$10 \leq M^2 \leq 20$	$1 \leq M'^2 \leq 3$
$\Lambda_c N^{(*)} D^*$	$5.71 \leq s_0 \leq 6.72$	$1.04 \leq s_0' \leq 1.99$	$2 \leq M^2 \leq 6$	$1 \leq M'^2 \leq 3$
$\Sigma_c N^{(*)} D^*$	$6.51 \leq s_0 \leq 7.62$	$1.04 \leq s_0' \leq 1.99$	$2 \leq M^2 \leq 6$	$1 \leq M'^2 \leq 3$

TABLE III. Parameters appearing in the fit function 1 of the coupling form factors related to the $\Lambda_b N^{(*)} B^*$ vertex.

	c_1	c_2	$c_3(\mathrm{GeV}^2)$
$g_1(Q^2)$	-2.44 ± 0.68	-0.34 ± 0.10	-17.88 ± 5.18
$g_2(Q^2)$	22.92 ± 6.64	3.87 ± 1.12	16.85 ± 4.89
$g_1^*(Q^2)$	-6.21 ± 1.73	-26.76 ± 8.01	-193.72 ± 56.17
$g_2^*(Q^2)$	88.27 ± 25.60	9.65 ± 2.70	24.32 ± 7.05

TABLE IV. Parameters appearing in the fit function 1 of the coupling form factors related to the $\Sigma_b N^{(*)} B^*$ vertex.

	c_1	c_2	$c_3(\mathrm{GeV}^2)$
$g_1(Q^2)$	297.08 ± 89.12	-282.66 ± 81.97	-225.11 ± 67.53
$g_2(Q^2)$	-18.12 ± 5.07	-3.82 ± 1.14	14.06 ± 4.08
$g_1^*(Q^2)$	87.60 ± 25.40	-82.34 ± 23.87	-24.88 ± 7.21
$g_2^*(Q^2)$	31.80 ± 9.22	0.90 ± 0.26	-6.70 ± 1.94

TABLE V. Parameters appearing in the fit function 1 of the coupling form factors related to the $\Lambda_c N^{(*)} D^*$ vertex.

	c_1	c_2	$c_3(\mathrm{GeV}^2)$
$g_1(Q^2)$	1.28 ± 0.36	0.92 ± 0.27	-155.98 ± 45.24
$g_2(Q^2)$	3.88 ± 1.13	1.27 ± 0.38	3.60 ± 1.04
$g_1^*(Q^2)$	3.01 ± 0.87	$(17.97 \pm 5.21)10^{-4}$	-2.77 ± 0.80
$g_2^*(Q^2)$	11.52 ± 3.23	-2.38 ± 0.71	2.26 ± 0.66

TABLE VI. Parameters appearing in the fit function 1 of the coupling form factors related to the $\Sigma_c N^{(*)} D^*$ vertex.

	c_1	c_2	$c_3(\mathrm{GeV}^2)$
$g_1(Q^2)$	-6.94 ± 2.01	11.18 ± 3.35	8.30 ± 2.41
$g_2(Q^2)$	-4.64 ± 1.35	$-(1.41 \pm 0.4)10^{-2}$	1.53 ± 0.45
$g_1^*(Q^2)$	26.37 ± 7.65	-23.18 ± 6.49	-11.03 ± 3.20
$g_2^*(Q^2)$	15.47 ± 4.48	2.22 ± 0.67	-6.34 ± 1.84

TABLE VII. Parameters appearing in the fit function 2 of the coupling form factors for $\Lambda_b N^{(*)} B^*$ vertex.

	g_0	a	b
$g_1(Q^2)$	-2.79 ± 0.81	0.21 ± 0.06	-0.19 ± 0.05
$g_2(Q^2)$	26.79 ± 8.03	-0.27 ± 0.07	-0.18 ± 0.05
$g_1^*(Q^2)$	-32.97 ± 9.89	0.13 ± 0.04	0.013 ± 0.003
$g_2^*(Q^2)$	97.93 ± 29.37	-0.13 ± 0.04	-0.07 ± 0.02

TABLE VIII. Parameters appearing in the fit function 2 of the coupling form factors for $\Sigma_b N^{(*)} B^*$ vertex.

	g_0	a	b
$g_1(Q^2)$	14.42 ± 4.32	-2.45 ± 0.71	8.18 ± 2.37
$g_2(Q^2)$	-21.93 ± 6.58	-0.35 ± 0.09	-0.21 ± 0.06
$g_1^*(Q^2)$	11.81 ± 3.54	-3.61 ± 1.05	4.95 ± 1.39
$g_2^*(Q^2)$	32.71 ± 9.81	0.13 ± 0.04	-0.20 ± 0.06

TABLE IX. Parameters appearing in the fit function 2 of the coupling form factors for $\Lambda_c N^{(*)} D^*$ vertex.

	g_0	a	b
$g_1(Q^2)$	2.26 ± 0.63	-0.31 ± 0.09	-1.55 ± 0.46
$g_2(Q^2)$	5.12 ± 1.53	-0.31 ± 0.09	-0.09 ± 0.03
$g_1^*(Q^2)$	3.32 ± 0.99	-0.17 ± 0.05	-0.08 ± 0.02
$g_2^*(Q^2)$	8.89 ± 2.49	0.69 ± 0.19	0.64 ± 0.19

TABLE X. Parameters appearing in the fit function 2 of the coupling form factors for $\Sigma_c N^{(*)} D^*$ vertex.

	g_0	a	b
$g_1(Q^2)$	4.23 ± 1.23	-1.80 ± 0.54	6.72 ± 2.02
$g_2(Q^2)$	-4.69 ± 1.31	-0.08 ± 0.02	-0.19 ± 0.06
$g_1^*(Q^2)$	1.66 ± 0.46	53.52 ± 14.98	-342.74 ± 95.97
$g_2^*(Q^2)$	17.98 ± 5.03	0.05 ± 0.01	-0.11 ± 0.03

TABLE XI. Parameters appearing in the fit function 3 of the coupling form factors for $\Lambda_b N^{(*)} B^*$ vertex.

	B_0	$B_1(\mathrm{GeV}^{-2})$	$B_2(\mathrm{GeV}^{-4})$
$g_1(Q^2)$	-2.79 ± 0.81	$(-18.65 \pm 5.59)10^{-3}$	$(-7.02 \pm 2.11)10^{-4}$
$g_2(Q^2)$	26.78 ± 8.02	-0.22 ± 0.06	$(5.23 \pm 1.50)10^{-3}$
$g_1^*(Q^2)$	-32.97 ± 9.89	-0.14 ± 0.05	$(-3.66 \pm 1.10)10^{-4}$
$g_2^*(Q^2)$	97.92 ± 29.36	-0.39 ± 0.11	$(6.66 \pm 1.86)10^{-3}$

TABLE XII. Parameters appearing in the fit function 3 of the coupling form factors for $\Sigma_b N^{(*)} B^*$ vertex.

	B_0	$B_1(\text{GeV}^{-2})$	$B_2(\text{GeV}^{-4})$
$g_1(Q^2)$	14.41 ± 4.30	-1.25 ± 0.37	$(-2.85 \pm 1.01)10^{-3}$
$g_2(Q^2)$	-21.94 ± 6.59	0.27 ± 0.08	$(-9.25 \pm 2.77)10^{-3}$
$g_1^*(Q^2)$	5.25 ± 1.57	-3.28 ± 0.95	-0.06 ± 0.02
$g_2^*(Q^2)$	32.43 ± 9.52	0.17 ± 0.05	$(16.45 \pm 4.93)10^{-3}$

TABLE XIII. Parameters appearing in the fit function 3 of the coupling form factors for $\Lambda_c N^{(*)} D^*$ vertex.

	B_0	$B_1(\text{GeV}^{-2})$	$B_2(\text{GeV}^{-4})$
$g_1(Q^2)$	2.20 ± 0.61	$(6.27 \pm 1.88)10^{-3}$	$(-1.10 \pm 0.33)10^{-5}$
$g_2(Q^2)$	5.13 ± 1.54	-0.31 ± 0.09	0.03 ± 0.01
$g_1^*(Q^2)$	3.10 ± 0.93	$(-24.94 \pm 7.84)10^{-3}$	$(2.33 \pm 6.99)10^{-4}$
$g_2^*(Q^2)$	9.03 ± 2.53	0.97 ± 0.27	-0.11 ± 0.03

TABLE XIV. Parameters appearing in the fit function 3 of the coupling form factors for $\Sigma_c N^{(*)} D^*$ vertex.

	B_0	$B_1(\text{GeV}^{-2})$	$B_2(\text{GeV}^{-4})$
$g_1(Q^2)$	4.22 ± 1.21	-1.44 ± 0.40	0.11 ± 0.03
$g_2(Q^2)$	-4.86 ± 1.41	0.16 ± 0.05	-0.04 ± 0.01
$g_1^*(Q^2)$	1.40 ± 0.42	-1.37 ± 0.38	-0.19 ± 0.06
$g_2^*(Q^2)$	17.46 ± 5.24	0.39 ± 0.12	0.04 ± 0.01

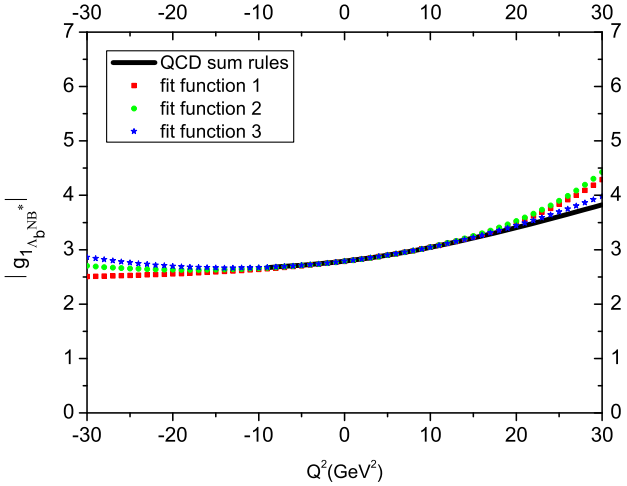

FIG. 2 (color online). $g_{1_{\Lambda_b NB*}}(Q^2)$ as a function of Q^2 at average values of the continuum thresholds and Borel mass parameters.

different fit functions. These small differences in the central values mainly belong to the fit function 3 and the strong coupling constant g_2. By considering the uncertainties in the results we can say that the numerical values of different strong coupling constants corresponding to various vertices obtained via different fit functions are roughly consistent with each other and are roughly independent from the choices of the fit functions. The maximum value belongs to the coupling constant g_2^* associated with the vertex

TABLE XV. Values of the strong coupling constants for the vertices under consideration for fit function 1.

Vertex	$\lvert g_1(Q^2=-m_{\mathcal{M}}^2)\rvert$	$\lvert g_2(Q^2=-m_{\mathcal{M}}^2)\rvert$	$\lvert g_1^*(Q^2=-m_{\mathcal{M}}^2)\rvert$	$\lvert g_2^*(Q^2=-m_{\mathcal{M}}^2)\rvert$
$\Lambda_b N^{(*)} B^*$	2.51 ± 0.75	43.73 ± 13.11	29.32 ± 8.78	119.26 ± 35.77
$\Sigma_b N^{(*)} B^*$	47.87 ± 14.35	46.83 ± 14.04	61.25 ± 18.37	31.81 ± 9.54
$\Lambda_c N^{(*)} D^*$	2.05 ± 0.61	7.78 ± 2.33	3.01 ± 0.90	2.60 ± 0.78
$\Sigma_c N^{(*)} D^*$	11.21 ± 3.36	4.64 ± 1.39	10.29 ± 3.08	16.65 ± 4.99

TABLE XVI. Values of the strong coupling constants for the vertices under consideration for fit function 2.

Vertex	$\lvert g_1(Q^2=-m_{\mathcal{M}}^2)\rvert$	$\lvert g_2(Q^2=-m_{\mathcal{M}}^2)\rvert$	$\lvert g_1^*(Q^2=-m_{\mathcal{M}}^2)\rvert$	$\lvert g_2^*(Q^2=-m_{\mathcal{M}}^2)\rvert$
$\Lambda_b N^{(*)} B^*$	2.68 ± 0.77	43.58 ± 13.07	29.17 ± 8.68	117.55 ± 32.91
$\Sigma_b N^{(*)} B^*$	45.67 ± 13.71	49.05 ± 13.74	59.58 ± 17.28	35.12 ± 10.54
$\Lambda_c N^{(*)} D^*$	2.41 ± 0.75	7.22 ± 2.17	4.03 ± 1.17	3.66 ± 1.10
$\Sigma_c N^{(*)} D^*$	10.51 ± 3.15	5.46 ± 1.53	8.97 ± 2.69	18.25 ± 5.29

TABLE XVII. Values of the strong coupling constants for the vertices under consideration for fit function 3.

Vertex	$\lvert g_1(Q^2=-m_{\mathcal{M}}^2)\rvert$	$\lvert g_2(Q^2=-m_{\mathcal{M}}^2)\rvert$	$\lvert g_1^*(Q^2=-m_{\mathcal{M}}^2)\rvert$	$\lvert g_2^*(Q^2=-m_{\mathcal{M}}^2)\rvert$
$\Lambda_b N^{(*)} B^*$	2.82 ± 0.87	37.35 ± 10.47	29.36 ± 8.81	114.38 ± 32.03
$\Sigma_b N^{(*)} B^*$	47.64 ± 13.81	37.15 ± 11.14	53.17 ± 15.42	40.89 ± 12.27
$\Lambda_c N^{(*)} D^*$	2.18 ± 0.65	6.77 ± 2.03	3.23 ± 0.97	3.40 ± 1.02
$\Sigma_c N^{(*)} D^*$	11.71 ± 3.51	6.11 ± 1.83	8.90 ± 2.67	16.51 ± 4.95

$\Lambda_b N^* B^*$, and the minimum value corresponds to the coupling g_1 related to the $\Lambda_c N D^*$ vertex for all fit functions.

In conclusion, we calculated the values of the strong coupling constants related to the vertices $\Lambda_b N B^*$, $\Lambda_b N^* B^*$, $\Sigma_b N B^*$, $\Sigma_b N^* B^*$, $\Lambda_c N D^*$, $\Lambda_c N^* D^*$, $\Sigma_c N D^*$, and $\Sigma_c N^* D^*$ in the framework QCD sum rules. We used different fit functions to extrapolate the results to the regions of Q^2 where the strong coupling constants under consideration are calculated. It has been found that the results are roughly independent of the choices of the fit functions for all the vertices. Our results may be checked via other nonperturbative approaches. The presented results can be helpful in explaining different exotic events observed via different experiments. These results may also be useful in the analysis of the results of heavy ion collision experiments as well as in exact determinations of the modifications in the masses, decay constants, and other parameters of the B^* and D^* mesons in the nuclear medium.

ACKNOWLEDGMENTS

This work has been supported in part by the Scientific and Technological Research Council of Turkey (TUBITAK) under Grant No. 114F018.

[1] N. Mathur, R. Lewis, and R. M. Woloshyn, Phys. Rev. D **66**, 014502 (2002).
[2] D. Ebert, R. N. Faustov, and V. O. Galkin, Phys. Rev. D **72**, 034026 (2005).
[3] J. L. Rosner, Phys. Rev. D **75**, 013009 (2007).
[4] M. Karliner and H. J. Lipkin, Phys. Lett. B **660**, 539 (2008).
[5] X. Liu, H. X. Chen, Y. R. Liu, A. Hosaka, and S. L. Zhu, Phys. Rev. D **77**, 014031 (2008).
[6] F. O. Durães, F. S. Navarra, and M. Nielsen, Phys. Lett. B **498**, 169 (2001).
[7] T. M. Aliev, A. Ozpineci, and M. Savci, Phys. Rev. D **65**, 096004 (2002).
[8] B. Julia-Diaz and D. O. Riska, Nucl. Phys. **A739**, 69 (2004).
[9] S. Scholl and H. Weigel, Nucl. Phys. **A735**, 163 (2004).
[10] A. Faessler, Th. Gutsche, M. A. Ivanov, J. G. Körner, V. E. Lyubovitskij, D. Nicmorus, and K. Pumsa-ard, Phys. Rev. D **73**, 094013 (2006).
[11] H.-Y. Cheng and C.-K. Chua, Phys. Rev. D **75**, 014006 (2007).
[12] C. S. An, Nucl. Phys. **A797**, 131 (2007); **A801**, 82(E) (2008).
[13] B. Patel, A. K. Rai, and P. C. Vinodkumar, J. Phys. G **35**, 065001 (2008); J. Phys. Conf. Ser. **110**, 122010 (2008).
[14] P.-Z. Huang, H.-X. Chen, and S.-L. Zhu, Phys. Rev. D **80**, 094007 (2009).
[15] Z.-G. Wang, Eur. Phys. J. A **44**, 105 (2010); Phys. Rev. D **81**, 036002 (2010).
[16] T. M. Aliev, K. Azizi, and M. Savci, Phys. Lett. B **696**, 220 (2011).
[17] A. Khodjamirian, Ch. Klein, Th. Mannel, and Y.-M. Wang, J. High Energy Phys. 09 (2011) 106.
[18] E. Hernandez and J. Nieves, Phys. Rev. D **84**, 057902 (2011).
[19] T. Gutsche, M. A. Ivanov, J. G. Korner, V. E. Lyubovitskij, and P. Santorelli, Phys. Rev. D **90**, 114033 (2014).
[20] A. Hayashigaki, Phys. Lett. B **487**, 96 (2000).
[21] Z.-G. Wang and T. Huang, Phys. Rev. C **84**, 048201 (2011).
[22] Z.-G. Wang, Int. J. Mod. Phys. A **28**, 1350049 (2013).
[23] A. Kumar, Adv. High Energy Phys. **2014**, 549726 (2014).
[24] K. Azizi, N. Er, and H. Sundu, Eur. Phys. J. C **74**, 3021 (2014).
[25] Z.-G. Wang, arXiv:1501.05093v1.
[26] M. A. Shifman, A. I. Vainshtein, and V. I. Zakharov, Nucl. Phys. **B147**, 385 (1979); Nucl. Phys. **B147**, 448 (1979).
[27] S. Choe, M. K. Cheoun, and S. H. Lee, Phys. Rev. C **53**, 1363 (1996).
[28] K. Azizi, Y. Sarac, and H. Sundu, Phys. Rev. D **90**, 114011 (2014).
[29] K. Azizi, Y. Sarac, and H. Sundu, arXiv:1501.05084.
[30] L. J. Reinders, H. Rubinstein, and S. Yazaki, Phys. Rep. **127**, 1 (1985).
[31] B. L. Ioffe, Prog. Part. Nucl. Phys. **56**, 232 (2006).
[32] V. M. Belyaev and B. L. Ioffe, Sov. Phys. JETP **57**, 716 (1982); Phys. Lett. B **287**, 176 (1992).
[33] K. A. Olive (Particle Data Group), Chin. Phys. C **38**, 090001 (2014).
[34] P. Gelhausen, A. Khodjamirian, A. A. Pivovarov, and D. Rosenthal, Phys. Rev. D **88**, 014015 (2013).
[35] K. Azizi and N. Er, Eur. Phys. J. C **74**, 2904 (2014).
[36] K. Azizi and H. Sundu, Phys. Rev. D **91**, 093012 (2015).
[37] K. Azizi, M. Bayar, and A. Ozpineci, Phys. Rev. D **79**, 056002 (2009).
[38] Z.-G. Wang, Phys. Lett. B **685**, 59 (2010).